Journal of
Nanoscience and Nanotechnology
Vol. 11, 5657–5662, 2011

RESEARCH ARTICLE

Microfluidic Biosensor for β-Amyloid(1-42) Detection Using Cyclic Voltammetry

Kamrul Islam[1], You-Cheol Jang[1], Rohit Chand[1], Sandeep Kumar Jha[1], Hyun Ho Lee[2], and Yong-Sang Kim[1,3,*]

[1] Department of Nano Science and Engineering, Myongji University, Gyeonggi 449-728, Republic of Korea
[2] Department of Chemical Engineering, Myongji University, Gyeonggi 449-728, Republic of Korea
[3] Department of Electrical Engineering, Myongji University, Gyeonggi 449-728, Republic of Korea

Numerous studies have identified β-amyloid(1-42) protein (Aβ42) in the cerebrospinal fluid as a potential biomarker of Alzheimer's disease. It is of particular interest to establish the diagnosis before reaching the stage of clinical severity. The current methods for studying amyloid detection, however, is often time-consuming, expensive, and labor intensive, making the analytical process very slow. Thus, a critical need exists for an analytical system that would enable the rapid investigation of amyloid formation with a very small amount of amyloidogenic peptides and reagents. In our present work, we report a simple microfluidic biosensor to analyze very small quantities of Aβ42 peptide on gold surface that were modified with Au nano-particles onto the thiol groups of self-assembled 1,6-hexandithiol cross-linkers. The vital advantage of this method includes retaining the bioactivity and environment similar to nature for protein immobilization while using minimal amounts of reagents and highly sensitive detection.

Keywords: Microfluidic Biosensor, β-Amyloid(1-42), Cyclic Voltammetry.

1. INTRODUCTION

Alzheimer's disease (AD) is the most common form of dementia, among the elderly. A major pathological hallmark of AD is the formation of senile plaques consisting of β-amyloid (Aβ) aggregates in the brain tissues.[1,2] The major component of the amyloid plaques exists in two predominant forms: the 40-residue Aβ(1–40) and 42-residue Aβ(1–42). These peptides differ in the absence or presence of two extra C-terminal residues and are produced from the processing of a larger amyloid precursor protein (APP),[3] resulting from sequential cleavage by proteases named β- and γ-secretases.[4–6] Biochemical studies also suggest that the longer, 42-residue Aβ(1–42) is more pathogenic than the shorter 40-residue Aβ(1–40),[7] due to its greater *in vitro* tendency to aggregate and precipitate as amyloid.[8] In fact, the senile plaques probably appear many years prior to the detection of the cognitive symptoms of AD.[9,10] As a consequence, it might be possible within the aging population that people show signs of AD neuropathology but still have no detectable cognitive symptoms.

Despite the significance of amyloid formation, little research progress had been made due to the limited number of effective analytical methods and probably for the lack of any method to analyze the physiology of amyloid aggregation. A few attempts have been made in past for the development of new screening assay methods for β-amyloid, which included capillary electrophoresis,[11] mass spectrometry,[12] enzyme-linked immunosorbent assay (ELISA),[13] surface plasmon resonance spectrometry,[14] and cell-based assay,[15] yet these assay systems could not fully satisfy the required criteria for detection of amyloid plaque formation. Moreover, most of these methods were time-consuming, expensive and labor intensive, lasting from months to years, making the analytical process very slow.

Thus, it is critically important to develop an analytical system that can detect Aβ(1–42) amyloid concentration in its aggregate forming step which would be a more suitable candidate to predict Alzheimer's disease. Although, it is difficult to devise an analytical system for *in-vivo* operation, *in-vitro* microreactor coupled with suitable detection system can easily analyze the protein molecules. Such microfluidic reactors can be miniaturized in the form of microchips using soft-lithographic techniques.[16,17] The microchip should consume very small

*Author to whom correspondence should be addressed.

amount of amyloidogenic peptides, can expedite the reaction and detection and would require less manual labor compared with existing procedures followed in analysis of such proteins.

In this regard, we describe herein a scalable microreactor device architecture with integrated electrochemical sensors as an analytical system for monitoring of *in-vitro* Aβ(1–42) plaque formation. The crucial step of proposed method is the suitable immobilization of Aβ(1–42) peptide on the electrode surface. It is known that, adsorption of proteins onto bulk metal surfaces leads to their denaturation and loss of their bioactivity.[18] The additional modification of gold electrodes with colloidal gold nanoparticles is one of the best solutions to overcome above problems. It has been recently reported that proteins adsorbed onto colloidal Au retain their bioactivity.[19–21] The gold-nano particles have attracted a lot scientific attention due to their not only biocompatibility, but also for the other properties such as large surface area and efficient electron conducting features.[22–24] In the work presented, the gold electrodes were modified with Au nano-particles by self-assembly while using 1,6-hexanedithiol as cross-linkers. The self-assembly of colloidal gold provides an environment similar to nature for protein immobilization while retaining their bioactivity. Therefore, Aβ(1–42) peptide molecules were allowed to adsorb directly on the surface of colloidal Au. Subsequent electrochemical measurements were performed using cyclic voltammetry (CV) for monitoring of each step of gold electrode modification with Aβ(1–42) peptide. The redox behavior of a solution of $K_3[Fe(CN)_6]/K_4[Fe(CN)_6]$ was studied in presence of hexanedithiol, colloidal nanoparticles and with aggregated Aβ(1–42) peptide. Presence of these bulk materials over working electrode resulted in increase of double layer capacitance and hence reduced electrochemical behavior of test solution. This was used as the basis for determination of Aβ(1–42) peptide concentration.

2. EXPERIMENTAL DETAILS

2.1. Chemicals

1,6-Hexanedithiol, 20 nm colloidal gold, $K_3[Fe(CN)_6]$ and $K_4[Fe(CN)_6]$ were purchased from Sigma-Aldrich (St. Louis, Mo). Human β-amyloid(1–42) peptide was obtained from rPeptide Co. (Athens, GA). All other solvents and chemicals were of analytical grade. All solutions were prepared and diluted using double distilled deionized (DDI) water.

2.2. Design and Fabrication of the Microchip

The devices were fabricated using standard photolithographic techniques (Fig. 1). The photo mask for fabrication of microchannel was designed with AutoCAD software (Autodesk, USA). The chip consisted of two reservoirs

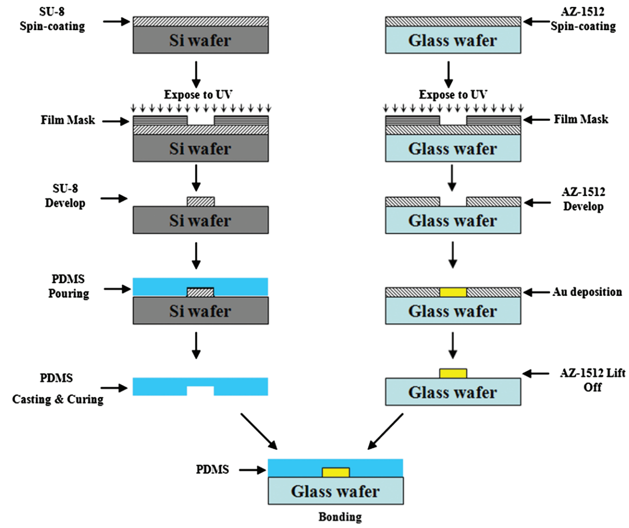

Fig. 1. Schematics of the fabrication process for the microchip.

acting as inlet and outlet along with a microchannel made from PDMS. The dimensions of each microchannel were 200 μm (width) $\times$ 200 μm (height) $\times$ 5.5 cm (length). The configuration of the microfluidic chip is shown in Figure 2. For fabrication of microchannels, 200 μm-thick photoresist (SU-8 50) was spin-coated and patterned on the silicon wafer. The height of the positive pattern on the molding master was 200 μm, which was equal to the channel depth created on the PDMS layer. PDMS was chosen as the channel material because of its inertness with the reagents and transparency for easy observation of amyloid formation. The PDMS layer was fabricated by pouring a degassed mixture of Sylgard 184 silicone elastomer and curing agent (10:1) onto a molding master, followed by curing for at least 1 h at 72 °C. The cured PDMS was separated from the mold, and reservoirs were made at the end

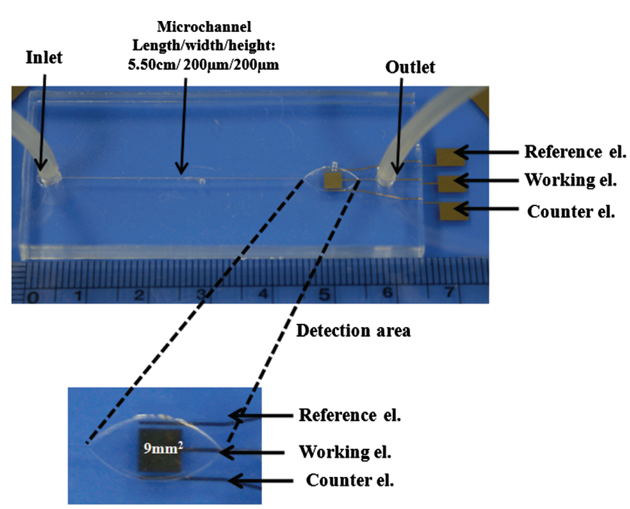

Fig. 2. The microfluidic chip showing gold microelectrodes (el.), microchannel, reservoirs, inlet, outlet and detection area.

of each channel using a 3-mm circular punch. At the same time, gold electrodes were fabricated on a glass substrate using standard photolithographic methods.

The three electrodes namely working, reference and counter electrodes were fabricated by thermal evaporation at the detection area. The size of the working electrode in the detection area was 3 mm in length as well as width. Other two electrodes were fabricated adjacent to the working electrode having a gap of 250 μm.

Bonding of PDMS layer on glass substrate containing the electrodes was performed with UV-Ozone cleaner to get improved bond strength.[25] When needed, the working electrode on the glass slides was modified with 1,6-hexanedithiol solution before bonding so as to avoid modification of other electrodes with this solution.

2.3. Surface Modification of the Electrode

The surface modification of gold electrode is shown in Figure 3. Clean working electrode was modified with 10 mM 1,6-hexanedithiol solution in ethanol by placing 3 μl of liquid over it and incubating at room temperature under humid condition in a closed petri plate for 3 h. It was washed with ethanol and the substrate was bonded with PDMS. The working electrode was then modified with 20 nm colloidal gold solution for 18 h under stationary condition. In subsequent steps, microfluidic condition was maintained in the microchannel using a precision pump (KD Scientific, USA) at 5 μl/min flow rate and electrodes were cleaned repeatedly with DDI water and ethanol using same condition. As a stock, 500 μM Aβ(1–42) peptide dissolved in 0.02% NH_4OH were prepared and kept at 4 °C. The test sample was diluted with Aβ assay buffer (20 mM phosphate buffer, pH 7.2 containing 100 mM NaCl) from stock solution just before treatment to avoid the Aβ aggregation. A 100 μL of the above solution was injected in the microchannel for deposition on the surface of electrodes modified by colloidal Au. Next, the electrodes were kept overnight in darkness at 4 °C under stationary condition. After deposition of Aβ(1–42) peptide, the electrodes were washed and stored at 4 °C in phosphate buffer (0.1 M KCl, 0.1 M KH_2PO_4, pH 7.2) until used for sensor measurements.

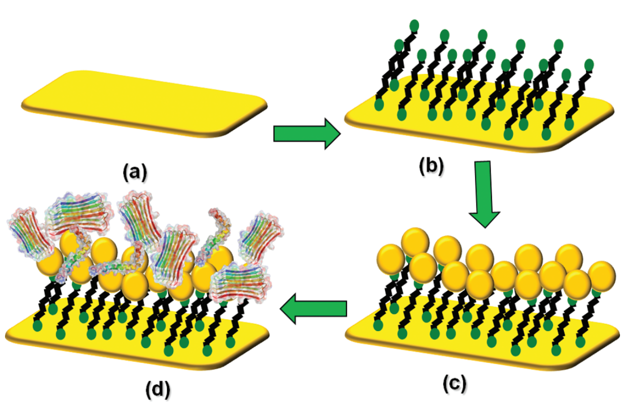

Fig. 3. Model of surface modification on gold electrode. a–b: self-assembly of 1,6 hexanedithiol as cross-linkers, c: 1,6-hexanditiol/Au-colloid modification, d: after deposition of Aβ(1–42) peptide.

2.4. Electrochemical Measurements

All electrochemical measurements including cyclic voltammetry (CV) were performed on the microfluidic chip using a CH Instruments (CHI model 800B) electrochemical analyzer under stationary liquid condition. At first, measurement was performed with bare electrode on the device and latter, upon each step of electrode modifications. Cyclic voltammetry (CV) was performed in 0.1 M Na_2HPO_4–NaH_2PO_4 buffer containing 1.0 mM $K_3[Fe(CN)_6]/K_4[Fe(CN)_6]$ and potential was cycled between +0.2 V to −0.6 V with a scan rate of 0.05 Vs^{-1}.

3. RESULTS AND DISCUSSION

3.1. Microfluidic Chip Operation

The study of amyloidogenic peptide aggregation remains most important factor in successful diagnosis of Alzheimer, as non-aggregated peptide is avirulent. Yet, only scant literature is available until date that studied amyloidogenic peptide aggregation. Meier et. al. studied on-chip peptide aggregation but rather focused on Aβ(1–40) peptide,[26] whereas Aβ(1–42) peptide is a more promising candidate for diagnosis of Alzheimer.[7] The group also did not attempt to measure the concentration of the peptide. Therefore, in the present study, we focused on aggregation as well as detection of Aβ(1–42) peptide by employing indirect electrochemical method in a microreactor. In this perspective, we fabricated a microfluidic chip (Fig. 2) in addition to electrochemical detector on a glass substrate. The volume of the detection chamber was 27 mm^3, and the fluidic control of the analyte in and out of this chamber was achieved through capillary motion and precision pump. This kind of microfluidic fabrication is advantageous in several aspects. First, it allows hexanedithiol, gold nanoparticle and the amyloid peptides to be immobilized efficiently on the gold electrode and prevent from contamination, and thus supporting high quality, low-background electrochemical sensing. Second, a three-electrode set-up was integrated onto the chip, which is particularly useful, compared to the commercially available cells, in cases where only limited sample volumes are available. And last, the key microfluidic components in the chip are simple in design, inexpensive and easy to fabricate. The use of microfluidic components with low power consumption, along with the employment of the electrochemical detection, suggests that the proposed device can be operated as a handheld device in future.

3.2. Amyloid β(1–42) Peptide Immobilization on Colloidal Gold Modified Electrodes

In order to detect Aβ(1–42) peptide in the microfluidic chip the first concern was to immobilize the amyloid peptide on the chip. Earlier studies showed that it is hard to retain the bioactivity of proteins if it is absorbed onto bulk metal surface.[18] Instead, if it is adsorbed onto colloidal Au, then their bioactivity is well retained.[19–21] In addition, the colloidal Au nanoparticle provides larger surface area than the bulk metal surface.[27,28] Hence, the proposed method incorporated a hexanedithiol linker to bridge between the Au electrode surface and that of the colloidal Au nanoparticles. For the electrochemical detection, $K_3[Fe(CN)_6]/K_4[Fe(CN)_6]$ solution was used assuming that with each modification of the electrode by hexanedithiol, colloidal nanoparticle and peptides, there will be changes in peak currents for this widely used redox active solution. The $K_3[Fe(CN)_6]/K_4[Fe(CN)_6]$ solution will give its original peak on the metal surface, followed by reduced peak for hexanedithiol as it will act as an insulator on the surface. Again, when the colloidal nanoparticle will be immobilized, the peak current will return to its origin, and after the immobilization of the peptide, the peak-to-peak separation will be enhanced due to electrode passivation.

As expected, $K_3[Fe(CN)_6]/K_4[Fe(CN)_6]$ showed reversible behavior on a bare Au electrode (Fig. 4) with a peak-to-peak separation ΔEp of 45 mV. After the covalent attachment of 1,6-hexanedithiols, the shape of CV changes dramatically. 1,6- Hexanedithiol forms well-packed monolayer on the surface of gold electrode responsible for the electrode passivation. The reversibility of the system could be restored after immobilization of gold colloid on the layer of 1,6-hexanedithiols with a peak-to-peak separation ΔEp of 48 mV. The Au nano-particles provide the necessary conduction pathways and promote the electron transfer between the redox marker and electrode surface.[22–24] The insulating layer of 1,6-Hexanedithiol on the electrode introduced a barrier to the interfacial electron transfer. The deposition of gold colloid particles on the 1,6-hexanedithiol self-assembled monolayer (SAM) decreased the semicircle diameter, which indicated a lower electron transfer resistance at the electrode interface. The increase of electron-transfer kinetics on the electrode surface originated from the conductive Au colloidal layer.

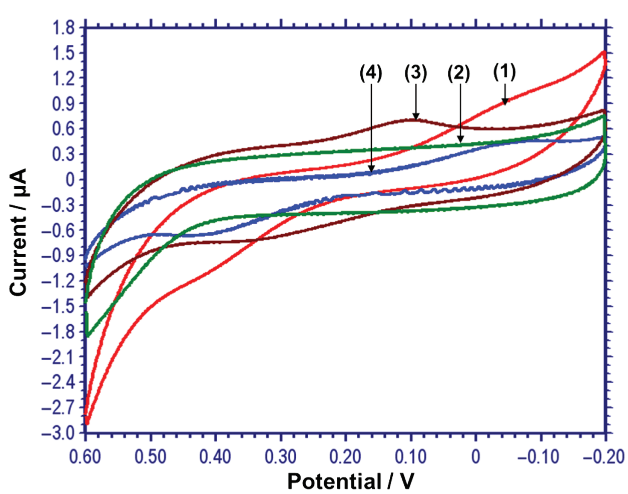

Fig. 4. Cyclic voltammogram of: (1) bare gold electrode; (2) 1,6-hexanedithiol modified electrode; (3) 1,6-hexanedithiol/Au-colloid modified electrode; (4) after deposition of Aβ(1–42) peptide. Solution composition: 0.1 M Na_2HPO_4–NaH_2PO_4 and 1.0 mM $K_3[Fe(CN)_6]/K_4[Fe(CN)_6]$ with scan rate 0.05 Vs^{-1}.

The immobilization of Aβ(1–42) peptide on the gold colloids was also monitored through CV. After deposition of Aβ(1–42) peptide, the interfacial electron transfer becomes inhibited, resulting in an increase in the electron transfer resistance due to formation of hydrophobic, more insulating layer of peptides on the electrode surface. This was reflected by increase in peak-to-peak separation ($\Delta E\text{p} = 51$ mV) in CV.

3.3. Assessment of Surface Morphology

We used Atomic Force Microscope (AFM) to determine three-dimensional surface morphologies of electrode after every modification steps and to study the interaction between Aβ(1–42) peptide and the other consecutive layers. For this purpose, the glass substrate was detached from the PDMS mold and subsequently rinsed with double distilled deionized water and dried with N_2 gas. AFM images were acquired on a PSIA XE 100 (Park Systems Co.) in non-contact mode with PPP-NCHR tips (silicon cantilever, Nanosensors Co.). The bare gold electrode was observed as smooth surface (Fig. 5(a)). After modification with 1,6-hexanedithiols, Au substrate showed a slight roughness due to the rearrangement of gold atoms via chemical reaction and due to introduction of linker molecules (Fig. 5(b)). The surface roughness increased after deposition of Au nanoparticles (Fig. 5(c)) and finally, the attachment of Aβ(1–42) peptide molecules was observed in Figure 5(d) with a higher surface roughness than the 1,6-hexanedithiol-modified surface. This confirmed the attachment of Au nanoparticle and Aβ(1–42) on the 1,6-hexanedithiol layer after incubation. The morphology of Aβ(1–42) was in the form of round aggregates with 10–100 nm diameter (Fig. 5(d)). The AFM observations indicated the affinity of Au nanoparticle to Aβ(1–42) peptides, and the aggregation properties of Aβ(1–42) peptides. The round shaped objects of Aβ(1–42) peptide is considered to be the self-assembling structure of ADDL (amyloid-derived diffusible ligands).

3.4. Calibration of the Sensor

Another objective in present study was to determine the concentration of Aβ(1–42) molecules effectively in order

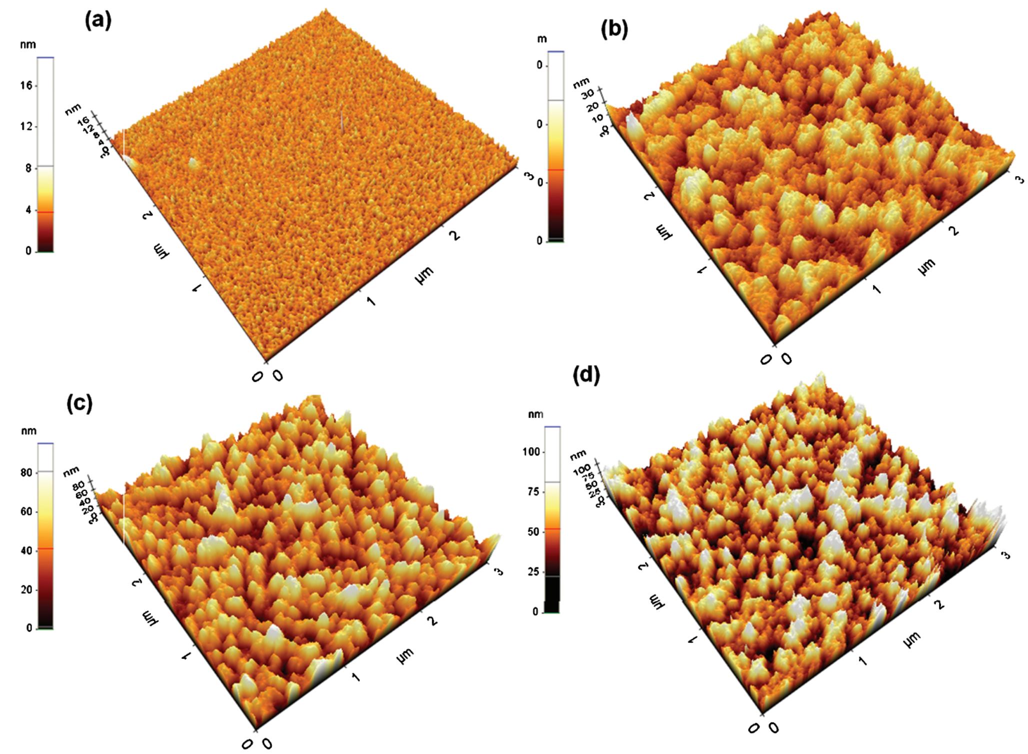

Fig. 5. AFM images of the bare gold substrate (a), after the immobilization of 1,6-hexanedithiol (b), after modified by gold nanoparticle on 1,6-hexanedithiol linker (c), and finally after the deposition of β-amyloid(1–42) protein.

to predict the onset of Alzheimer disease. For this purpose, different concentrations (10 μM, 50 μM, 100 μM, 200 μM, 300 μM, 350 μM, 400 μM) of Aβ(1–42) peptide were applied on the electrode and the CV signals were recorded. Figure 6 shows the effect of different concentrations of Aβ(1–42) on cyclic voltammetric response on the chip. As the concentration of Aβ(1–42) is increased from 10 μM to 400 μM, the peak current decreased correspondingly. There is a good sigmoidal relationship between the peak current and the concentration Aβ(1–42) in the entire

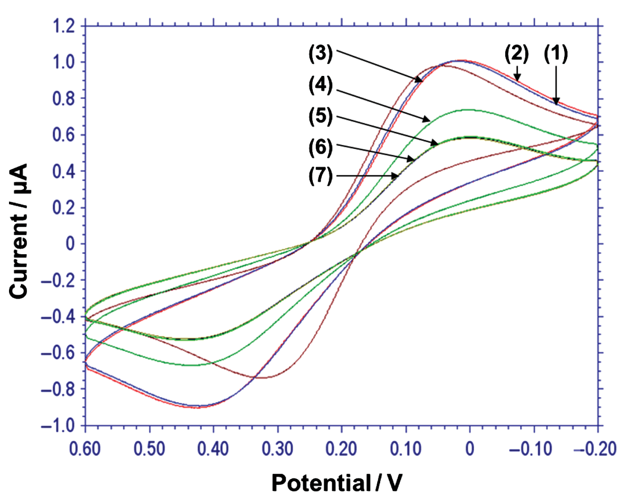

Fig. 6. Changes in the peak current for the different concentrations of β-amyloid(1–42) protein.

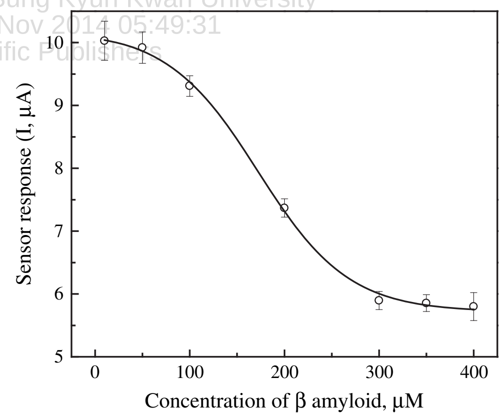

Fig. 7. Sensor calibration curve: sensor output versus β-amyloid concentrations.

concentration range studied in this case (Fig. 7). Each data in Figure 7 was an average value of three measurements. The linear detection range existed between 100 μM to 300 μM of Aβ(1–42). These experimental results were indicative of a successful working model for detection of amyloidogenic peptides on the fabricated microfluidic chip.

4. CONCLUSIONS

We have developed an electrochemical biosensor for the detection of Aβ(1–42) peptide in a microfluidic chip

architecture. The process used cyclic voltammetric study of redox behavior of $K_3[Fe(CN)_6]/K_4[Fe(CN)_6]$ on colloidal gold nanoparticle bound through 1,6- hexanedithiol linkers on gold working electrode. The modification of gold electrode with Au nanoparticles provided a suitable environment for stable immobilization of Aβ(1–42) keeping its bioactivity in microreactor environment. Aggregation of Aβ(1–42) peptide in increasing order of concentration resulted in passivation of working electrode and hence decreased the sensor output current. The proposed detection method could be a suitable diagnostic candidate for Alzheimer, if an additional layer of monoclonal antibody against Aβ(1–42) peptide be used to enhance selectivity of detection. This method shall be helpful in analyzing other important biomarker peptides of Alzheimer's disease such as Total tau, and Phospho-tau and can be effectively useful in detection of other protein molecules that are otherwise difficult to detect using conventional techniques due to loss of bioactivity.

Acknowledgments: This word was supported by Grant no. (ROA-2006-000-10274-0) from National Research Laboratory Program of the Korea Science and Engineering Foundation.

References and Notes

1. R. M. Murphy, *Annu. Rev. Biomed. Eng.* 4, 155 **(2002)**.
2. D. K. Lahiri, M. R. Farlow, N. H. Greig, and K. Sambamurti, *Drug Dev. Res.* 56, 267 **(2002)**.
3. J. Hardy, *Trends Neurosci.* 20, 154 **(1997)**.
4. S. G. Younkin, *J Physiol - Paris* 92, 289 **(1998)**.
5. D. J. Selkoe, *Physiol Rev* 81, 741 **(2001a)**.
6. D. J. Selkoe, *Neuron* 32, 177 **(2001b)**.
7. S. G. Younkin, *Ann Neurol* 37, 287 **(1995)**.
8. C. J. Barrow and M. G. Zagorski, *Science* 253, 179 **(1991)**.
9. H. Braak and E. Braak, *Neurobiology Aging* 18, 351 **(1997)**.
10. D. R. Thal, U. Rub, M. Orantoes, and H. Braak, *Neurology* 58, 1791 **(2002)**.
11. S. Sabella, M. Quaglia, C. Lanni, M. Racchi, S. Govoni, G. Caccialanza, A. Calligaro, V. Bellotti, and E. De Lorenzi, *Electrophoresis* 25, 3186 **(2004)**.
12. X. Cheng and R. B. van Breemen, *Anal. Chem.* 77, 7012 **(2005)**.
13. P. Inbar, M. R. Bautista, and S. A. Takayama, *J. Yang, Anal. Chem.* 80, 3502 **(2008)**.
14. J. Ryu, H.-A. Joung, M.-G. Kim, and C. B. Park, *Anal. Chem.* 80, 2400 **(2008)**.
15. B. L. Apostol, A. Kazantsev, S. Raffioni, K. Illes, J. Pallos, L. Bodai, N. Slepko, J. E. Bear, F. B. Gertler, S. Hersch, D. E. Housma, J. L. Marsh, and L. M. Thompson, *Proc. Natl. Acad. Sci.* 100, 5950 **(2003)**.
16. G.-S. Joo, S. K. Jha, and Y.-S. Kim, *Curr. Appl. Phys.* 9, e222 **(2009)**.
17. S. K. Jha, G.-S. Ra, G.-S. Joo, and Y.-S. Kim, *Curr. Appl. Phys.* 9, e301 **(2009)**.
18. M. Wang, L. Wang, G. Wang, X. Ji, Y. Bai, T. Li, S. Gong, and J. Li, *Biosens. Bioelectron.* 19, 575 **(2004)**.
19. Y. Liu, F. Yin, Y. Long, Z. Zhang, and S. Yao, *J. Colloid Interf. Sci.* 258, 75 **(2003)**.
20. S. Liu and H. Ju, *Biosens. Bioelectron.* 19, 177 **(2003)**.
21. C.-X. Li, K.-Q. Deng, G.-L. Shen, and R.-Q. Yu, *Anal. Sci.* 20, 1277 **(2004)**.
22. M. Lu, X. H. Li, B. Z. Yu, and H. L. Li, *J. Colloid Interf. Sci.* 248, 376 **(2002)**.
23. M. Yang and Z. Zhang, *Electrochim. Acta* 49, 5089 **(2004)**.
24. Ch.-Z. Li, Y. Liu, and J. H. T. Luong, *Anal. Chem.* 77, 478 **(2005)**.
25. J. H. Kim, C. J. Kang, and Y. S. Kim, *Microelectron. Eng.* 71, 119 **(2004a)**.
26. M. Meier, J. Kenney-Darling, S. H. Choi, E. M. Norstrom, S. S. Sisodia, and R. F. Ismagilov, *Angew. Chem. Int. Ed.* 48, 1487 **(2009)**.
27. S. Singha, H. Datta, and A. K. Dasgupta, *J. Nanosci. Nanotechnol.* 10, 826 **(2010)**.
28. R. R. Bhattacharjee, A. K. Das, D. Haldar, S. Si, A. Banerjee, and T. K. Mandal, *J. Nanosci. Nanotechnol.* 5, 1141 **(2005)**.

Received: 24 June 2010. Accepted: 27 January 2011.